This is a preprint of a paper intended for publication in a journal or proceedings. Since changes may be made before publication, this preprint is made available with the understanding that it will not be cited or reproduced without the permission of the author.

UCRL - 77082

Conf 751136--22

LAWRENCE LIVERMORE LABORATORY

University of California/Livermore, California

NOTICE

This report was prepared as an account of work sponsored by the United States Government. Neither the United States nor the United States Energy Research and Development Administration, nor any of their employees, nor any of their contractors, subcontractors, or their employees, makes any warranty, express or implied, or assumes any legal liability or responsibility for the accuracy, completeness or usefulness of any information, apparatus, product or process disclosed, or represents that its use would not infringe privately owned rights.

X-RAY MICROSCOPY OF LASER FUSION TARGETS IN FOUR ENERGY BANDS FROM 0.7 TO 4.0 keV

M. J. Boyle, F. D. Seward, T. L. Harper,
L. N. Koppel, K. J. Pettipiece, and H. G. Ahlstrom

October 15, 1975

MASTER

This Paper was Prepared for Submission to
the APS Meeting, St. Petersburg, Florida,
November 10-14, 1975

X-RAY MICROSCOPY OF LASER FUSION TARGETS IN FOUR ENERGY BANDS FROM 0.7 TO 4.0 keV

The ability to spatially resolve the x-ray emission from laser fusion targets is a vital diagnostic. Insight into the temperature and density distributions associated with the target implosion may be inferred from the nature of the continuum and line x-ray emission from these hot, dense laser produced plasmas. These spatial distributions may, in turn, be compared to the predicted profiles generated by the laser fusion computer codes, thereby, commenting on the applicability of the code physics used to model the target implosion problem.

Spatial imaging of the x-ray emission from laser fusion targets depends upon the principle of total reflection and the fact that the refractive index is less than one in the x-ray regime. Thus, at near grazing incidence, x-rays can be totally reflected from smooth surfaces (Figure 1). It may be demonstrated that for x-rays incident upon a cylindrical surface with a radius of curvature R, the reflective surface behaves as a cylindrical lens whose focal length is given by

$$f = \frac{R \sin i}{2}$$

where i is the grazing incidence angle. Thus, x-rays from a point source are reflected to a line image. Figure 2 illustrates the principles behind point-to-point x-ray imaging on which our present, simple, x-ray microscope is based. The introduction of a second reflecting surface of similar curvature and located orthogonal to the first mirror forms a point-to-point

Work performed under the auspices of the U.S. Energy Research & Development Administration under contract No. W-7405-Eng-48.

image of the source from the small fraction of incident rays reflected from both surfaces. The combination of two, orthogonal x-ray mirrors constitutes a single lens or channel of our x-ray microscope. Since, for a given grazing incidence angle, the spectral energy range over which total reflection occurs is a function of the reflecting surface material, simple multi-channel microscope operation is feasible. The multi-channel arrangement employed at Livermore is illustrated schematically in Figure 3. Four x-ray mirrors are arranged as illustrated forming a x-ray lens at each of the four corners of the array. Two of the corners are glass and two have nickel coatings on the glass substrate. Placing different k-edge filters in front of each lens makes each lens sensitive to a particular energy band. Thus, the instrument is capable of taking simultaneous pictures in four separate energy bands.

The properties of this x-ray microscope are summarized below.

Angle of incidence	=	1.0 deg
Mirror radius of curvature	=	19.7 m
Focal length	=	17.1 cm
Object distance	=	22.9 cm
Magnification	=	3
Subtended Solid Angle	=	2.3×10^{-7} str.
Energy bands centered at		0.8, 1.5, 2.5, 3.0 keV

In order to derive quantitative information from the x-ray microscope data recorded on film, the resolution and mirror reflection efficiency of the microscope and the calibration of the x-ray film must be known. Kodak type M double emulsion film was calibrated at several energies using a

Henke-tube x-ray source, a proportional counter to monitor the incident flux level and a Photometric Data Systems series 1000 microdensitometer. The film calibration curves are reproduced in Figure 5.

The x-ray emission from the glass microballoon laser fusion targets is intense enough so that the microscope system resolution is not limited by the grain size of the x-ray film. Determination of the spatial resolution of the instrument was accomplished by the standard procedure of photographing an opaque grid backlighted by a broad source of copper L x-rays. The grid consists of two superimposed pieces of 1000 line/inch mesh rotated slightly with respect to each other. The pattern seen in Figure 6 varies from the basic square grid pattern repeating at 25 μm intervals, to smaller wedge-shaped segments formed by two intersecting mesh lines. Figure 7 shows microdensitometer traces across two of these characteristic regions. In the regions of best focus, resolution between 3-5 μm are observed. The diameter of the best-focus region (better than 10 μm) is approximately 500 μm.

Reflection efficiency measurements on six glass and nickel surfaces were made between 1 and 3 keV. The experimental data for single reflections superimposed upon their theoretical reflection efficiency curves are presented in Figure 8. These data in conjunction with the transmission properties of nickel, aluminum and mylar filter pack combination yield the four energy channels response functions of the microscope (Figure 9). Energy channels centered at 0.8, 1.5, 2.5 and 3.0 keV are thereby defined. Knowledge of the energy channels response functions and the x-ray film

calibration now allows us to obtain quantitative emissivity data from micrographs of laser fusion targets.

To date, emissivity and spectral data have been obtained from the x-ray micrographs. Figure 10 shows a typical microshell laser fusion target, the focusing strategy employed in irradiating the target with the JANUS two-beam laser system and the resulting x-ray micrograph images which have undergone post processing color image enhancement. Two beams of 1.06 μm radiation focused through f/1 lenses irradiated the 75 μm diameter target filled with DT gas. The laser pulse was 62 ps FWHM wide with 13 joules/beam. Figure 11 presents the iso-emissivity contours derived from the PDS microdensitometer scan of the 0.8 keV channel image and the x-ray film calibration.

Furthermore, the emissivity contours associated with each of the four energy channel images may be integrated to yield absolute x-ray spectral data. Spectral data so derived is presented in Figure 12 along with spectral data derived from three independent techniques, all operative on the same shot. In addition, the spectral emission from only the central core of the imploded target has been computed for comparison. Experimental agreement among all the data is excellent.

In summary, a grazing incidence x-ray microscope has been shown able to photograph the x-ray emission from laser-produced plasmas between 0.8 and 4.0 keV with a spatial resolution of $\sim$ 3 microns. The calibration of the

x-ray mirror energy response functions and the x-ray film allow absolute measurements of the spatial and spectral distribution of the x-ray emission from laser fusion targets.

X-RAY REFLECTION AT GRAZING INCIDENCE

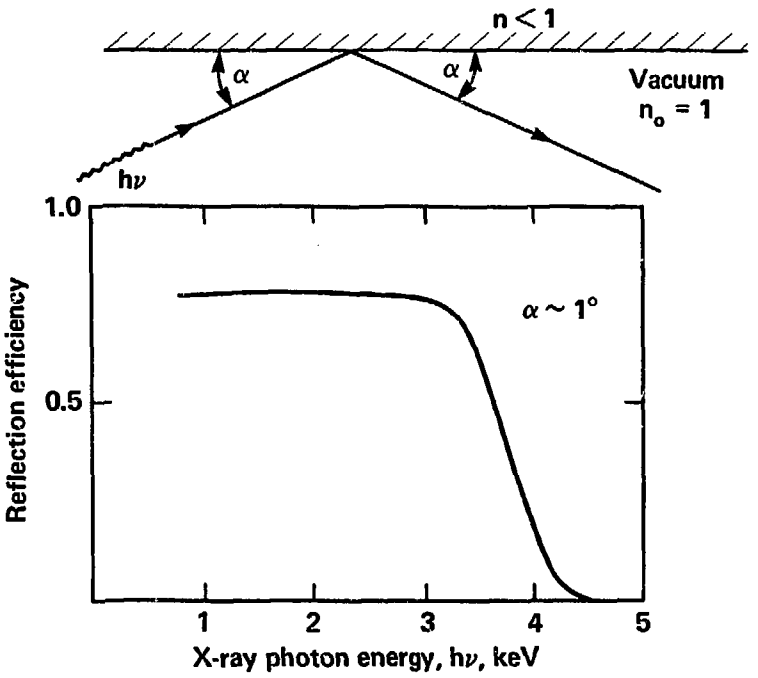

Figure 1

GRAZING INCIDENCE X-RAY FOCUSING PRINCIPLES

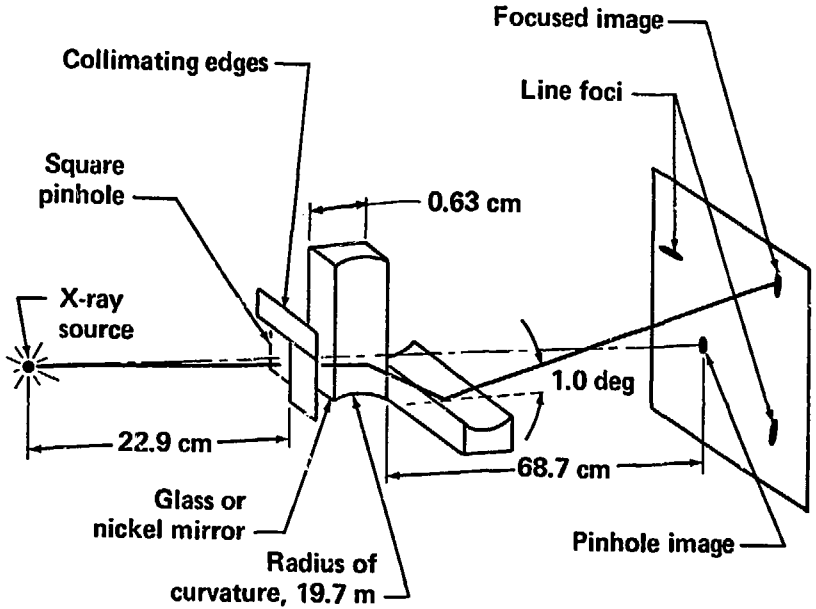

Figure 2

SIMPLE 4-CHANNEL X-RAY MICROSCOPE

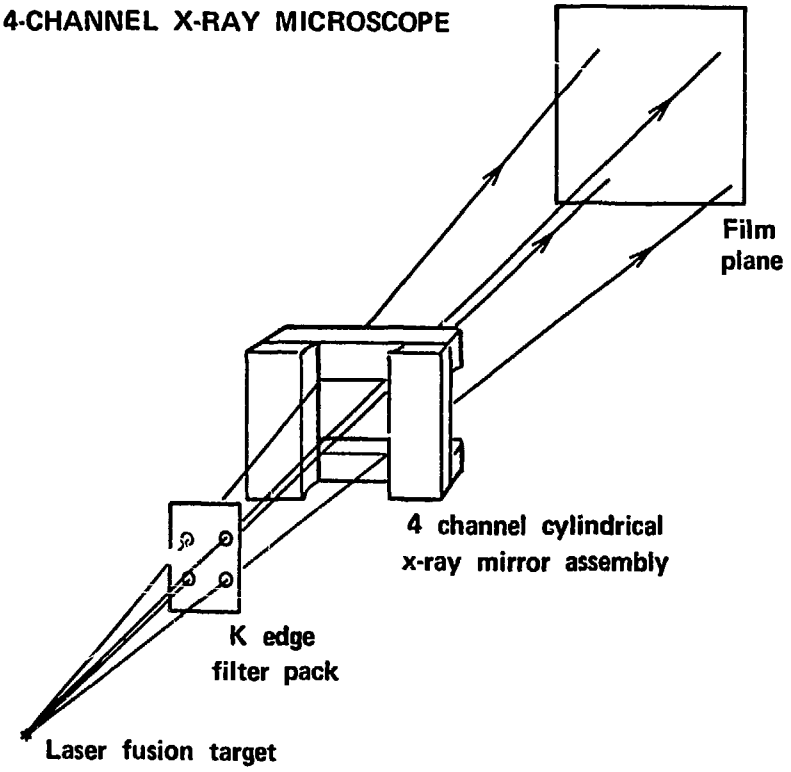

Figure 3

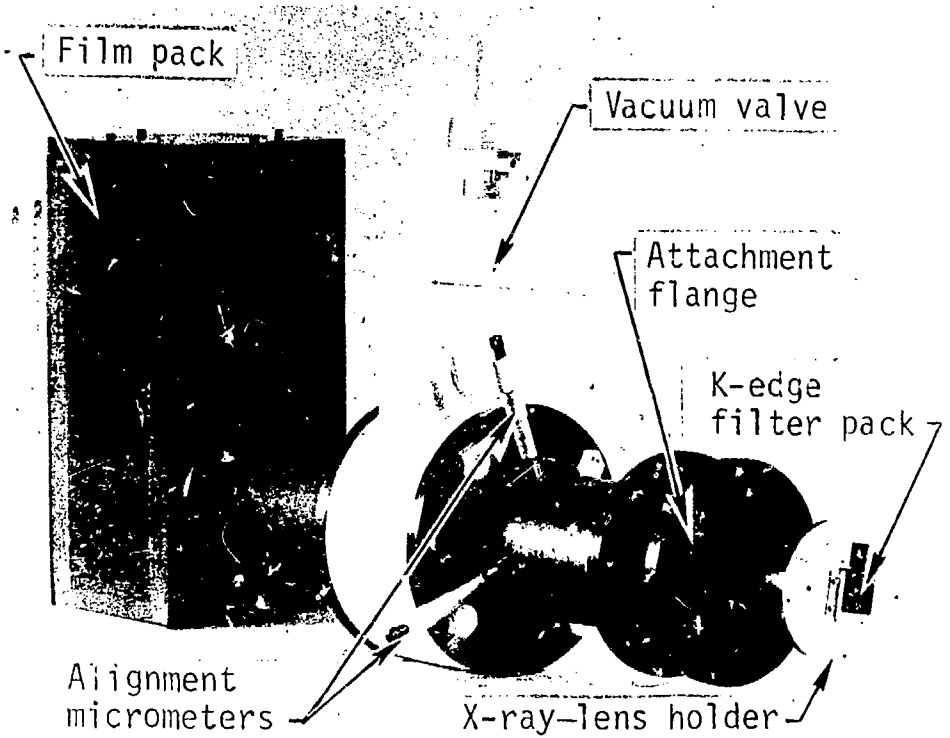

Four-Channel Microscope Assembly

Fig. 4

KODAK TYPE M X-RAY FILM CALIBRATION

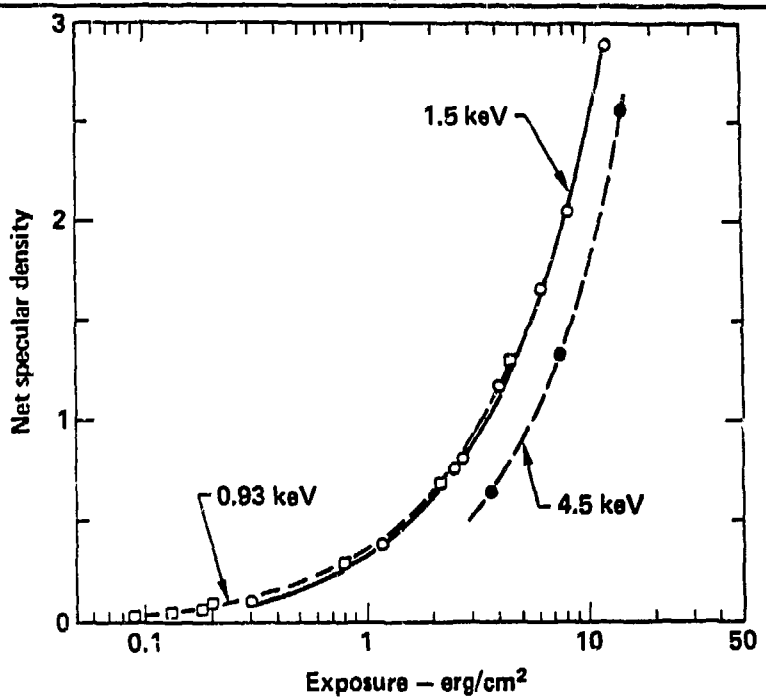

Taken from: Stoering and Toor, LLL Rept. UCID-16775 (1975)

Figure 5

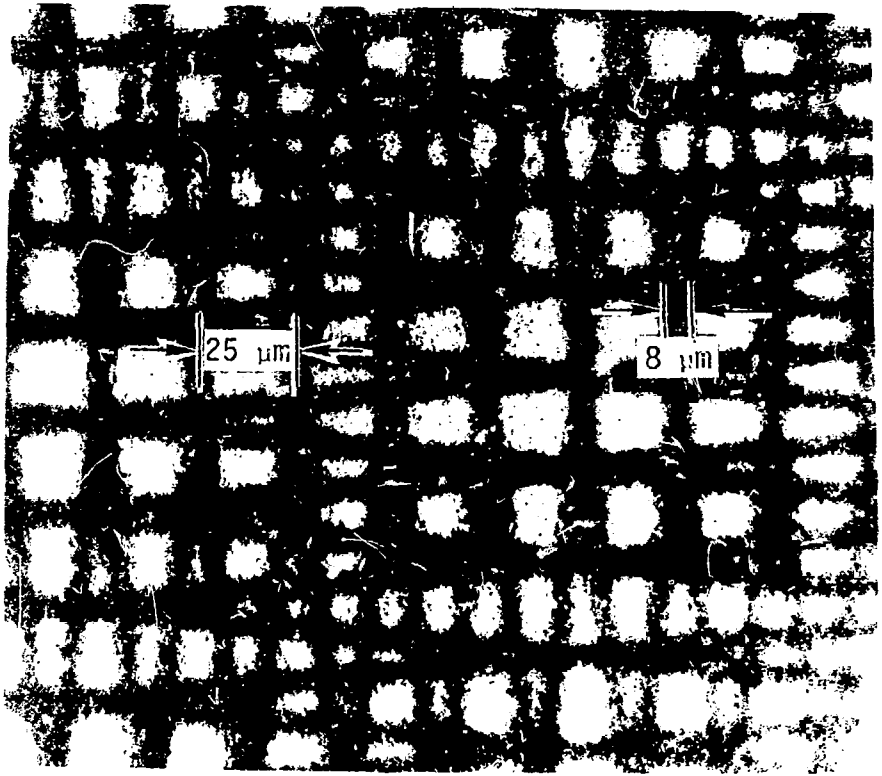

Resolution Grid

Figure 6

DENSITOMETER TRACES OF WIRE GRID

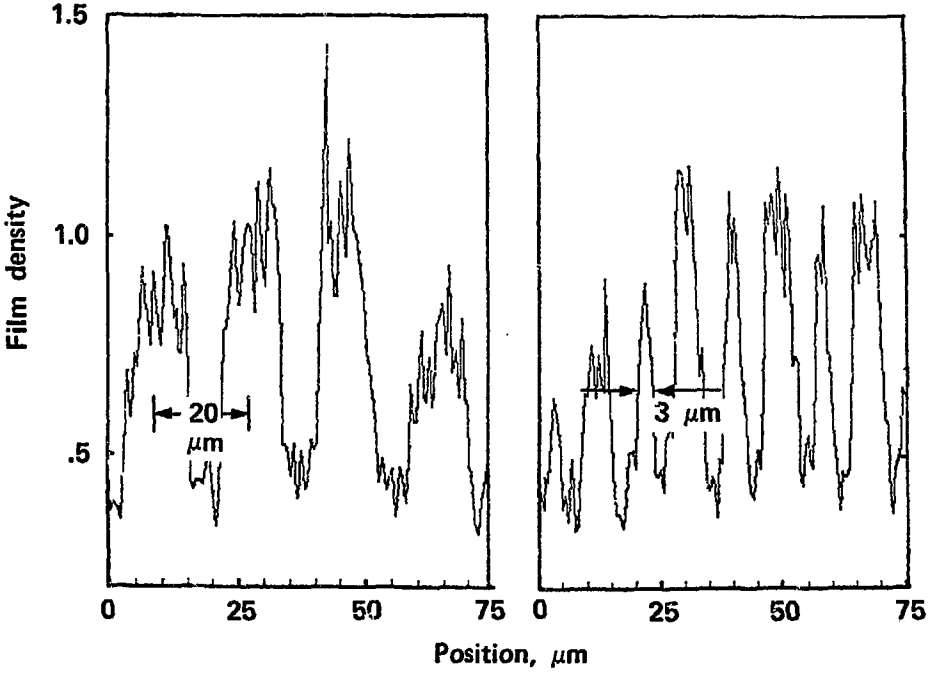

Figure 7

EXPERIMENTAL REFLECTION EFFICIENCIES OF X-RAY MIRRORS

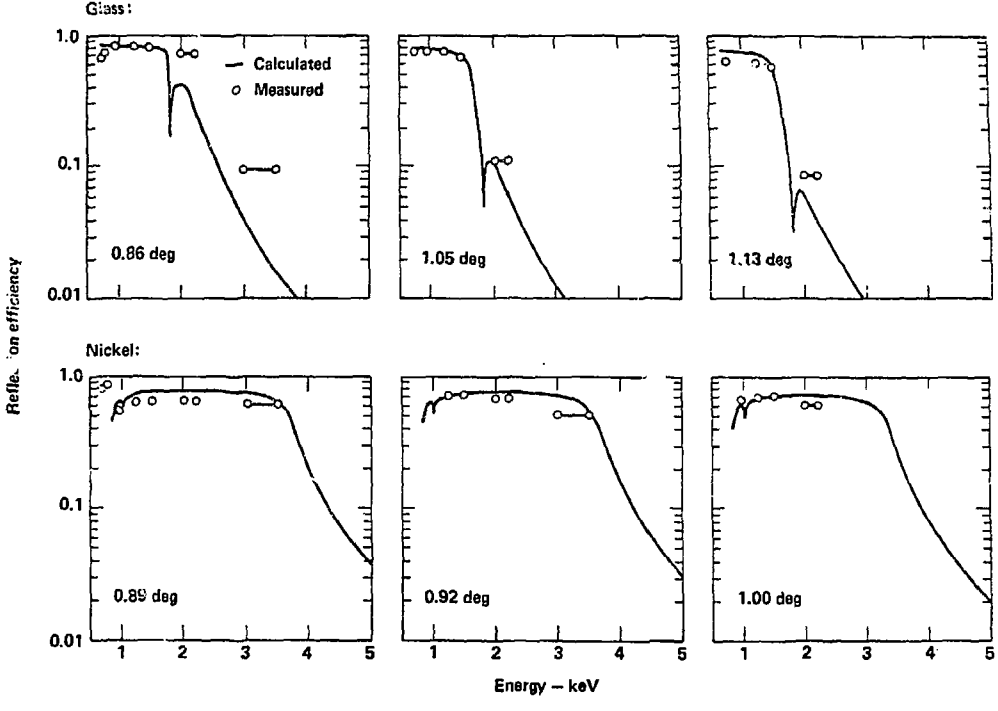

Figure 8

SPECTRAL RESPONSE FUNCTIONS OF THE FOUR CHANNEL X-RAY MICROSCOPE

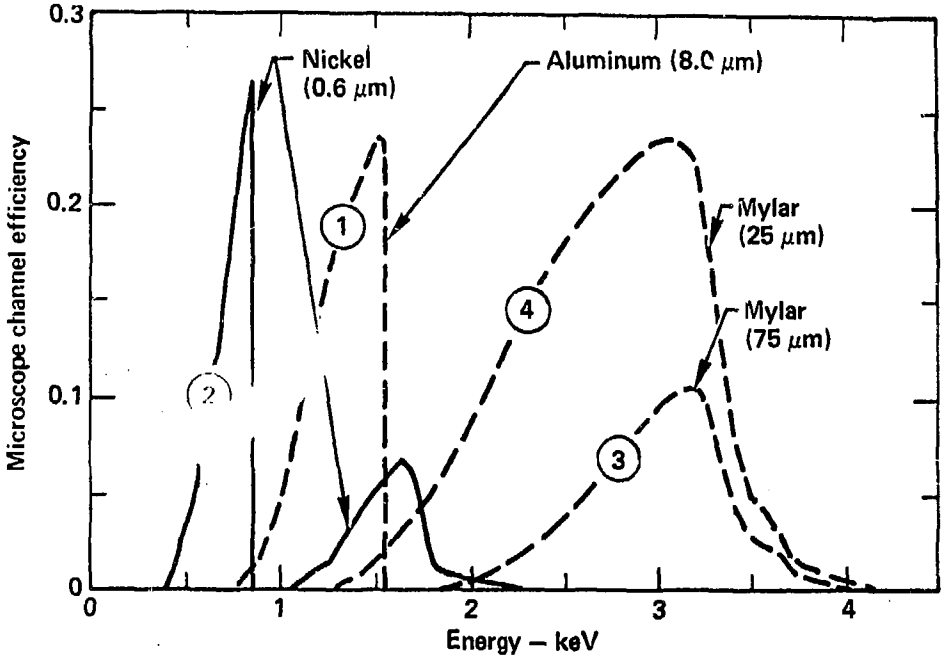

Figure 9

X-RAY MICROGRAPHS

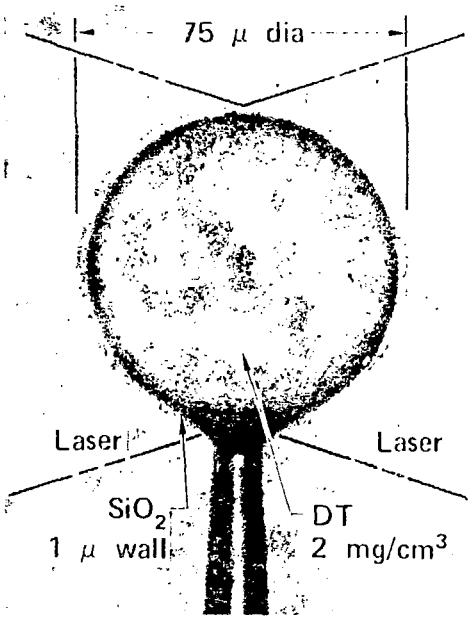

Target: B-17
Laser energy: 26.9 J
Laser pulse width: 62 ps
Neutron yield: 8.2 × 10^5

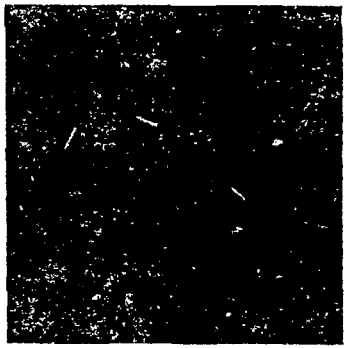

.8 keV microscope image

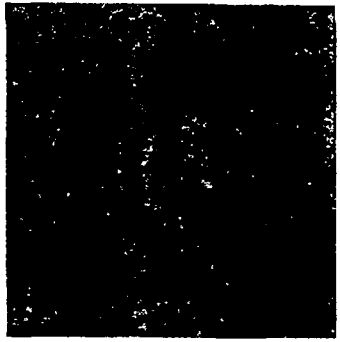

2.5 keV microscope image

Figure 10

Figure 11

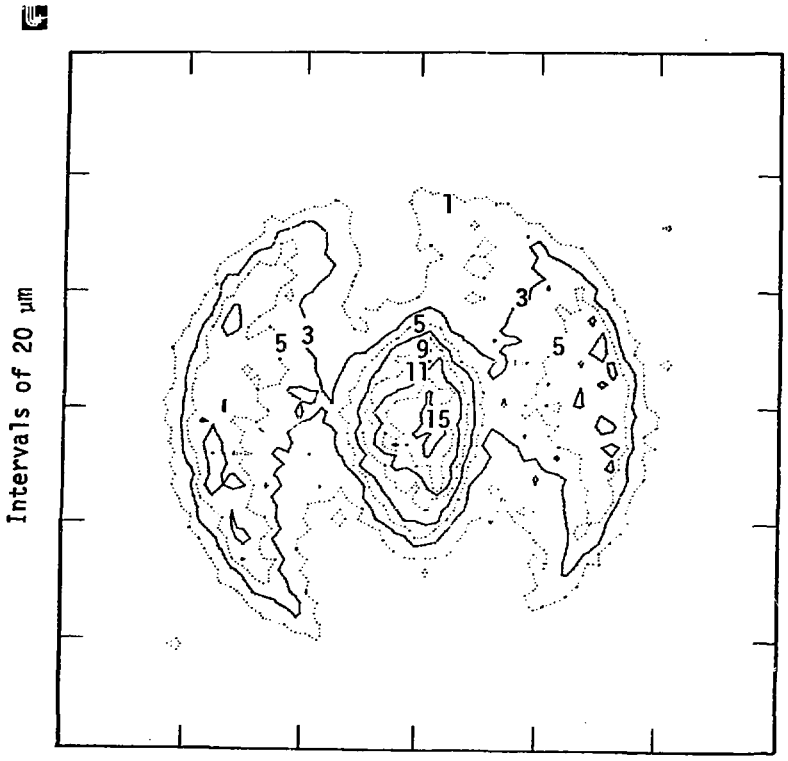

MICROSPHERE TARGET
Iso-emissivity (10^9 erg/cm^2) Contours

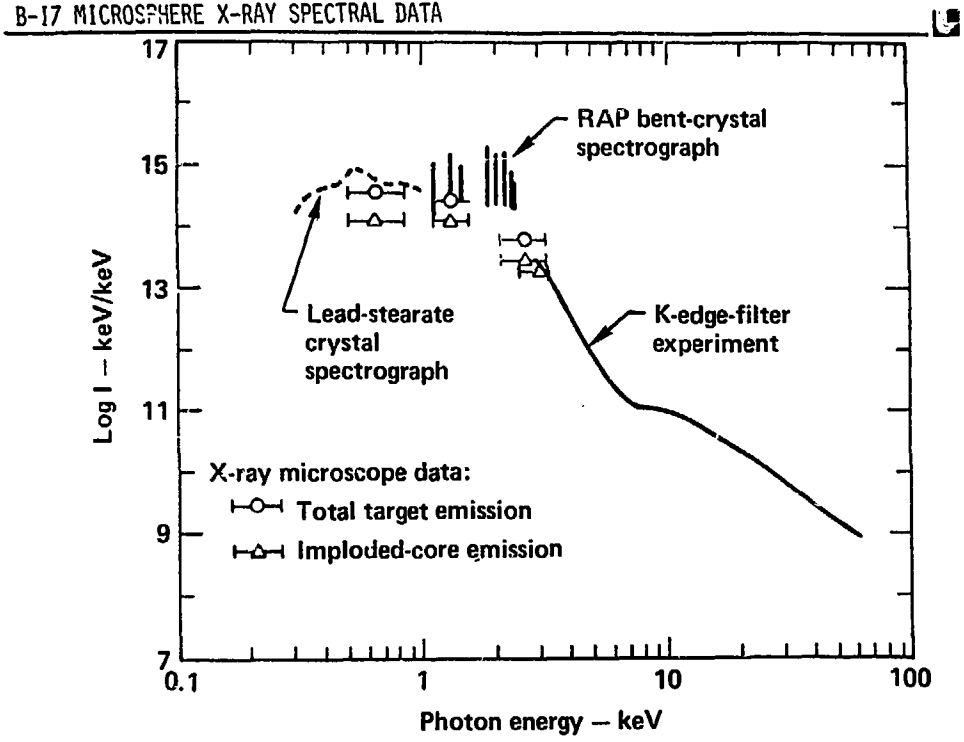
B-17 MICROSPHERE X-RAY SPECTRAL DATA
17
15
13
11
9
7
Log I – keV/keV
0.1
1
10
100
Photon energy – keV
RAP bent-crystal spectrograph
Lead-stearate crystal spectrograph
K-edge-filter experiment
X-ray microscope data:
Total target emission
Imploded-core emission

Figure 12